Showcasing research from the SZU-NUS Collaborative Innovation Center for Optoelectronic Science & Technology, Shenzhen University, China, and the Department of Chemistry, National University of Singapore, Singapore.

Polyquinoneimines for lithium storage: more than the sum of its parts

A straightforward synthetic strategy for the construction of electrode materials is demonstrated by the polymerization of two kinds of electrochemically active organic monomers without sacrificing specific capacity.

As featured in:

See Chenliang Su, Kian Ping Loh *et al.*, *Mater. Horiz.*, 2016, **3**, 429.

ROYAL SOCIETY OF CHEMISTRY

rsc.li/materials-horizons

Registered charity number: 207890

Materials Horizons

COMMUNICATION

View Article Online
View Journal | View Issue

Cite this: *Mater. Horiz.*, 2016, 3, 429

Received 15th March 2016,
Accepted 26th May 2016

DOI: 10.1039/c6mh00072j

www.rsc.li/materials-horizons

Polyquinoneimines for lithium storage: more than the sum of its parts†

Bingbing Tian,‡[ab] Guo-Hong Ning,‡[b] Wei Tang,[b] Chengxin Peng,[b] Dingyi Yu,[b] Zhongxin Chen,[b] Yinglin Xiao,[a] Chenliang Su*[ab] and Kian Ping Loh*[ab]

A straightforward synthetic strategy for the construction of electrode materials is demonstrated by the polymerization of two kinds of electrochemically active organic monomers without sacrificing specific capacity. Polyquinoneimines (PQIs), synthesised by the polycondensation reaction of 2,6-diaminoanthraquinone and the anhydrides, were used as a cathode in lithium ion batteries (LIBs). Electrochemical analysis such as CV and galvanostatic cycling reveals that PQIs exhibit the combined electrochemical properties of the two monomers. The mechanism of lithiation/delithiation of the PQIs has been investigated by means of electrochemical and spectroscopic (FTIR) analytical techniques. The as-prepared PQI-1 exhibits a higher specific capacity of 210 mA h g^{-1} and a better cycling performance (136 mA h g^{-1} after 200 cycles) compared with their polymeric precursors.

Conceptual insights

In this study, a redox-active organic molecule, 2,6-diaminoanthraquinone (DAAP), was selected as a linker to connect the anhydrides into polyquinoneimines (PQIs) *via* a facile wet-chemistry approach. As both quinones and anhydrides are electrochemically active, the direct polymerization of these two monomers did not introduce additional inactive monomers, thus minimizing the loss of theoretical specific capacity with respect to the molar mass increase. Furthermore, the increased molar mass effectively suppresses the dissolution of the active materials in the electrolyte. PQIs synthesized by this unique polymerization strategy can realize a high capacity as well as a good cycle stability, which makes PQIs a promising organic positive-electrode material for lithium ion batteries.

Introduction

Organic positive-electrode materials are attractive for lithium ion batteries (LIBs) due to their high theoretical capacities, sustainability, flexibility, low cost, environmental friendliness and safety.[1–6] Recently, organic carbonyl compounds such as quinones and anhydrides have attracted considerable attention as redox active molecules for energy storage.[7–15] However, the dissolution of the organic active materials in the electrolyte is a key obstacle to their application as electrode materials. In order to suppress dissolution, one approach is to use mesoporous carbon (*i.e.* carbon black,[16] graphene[17,18] or carbon nanotubes[19,20]) as well as a functionalized graphene nanocomposite[21] to immobilize the redox-active molecules, thus improving cycling performance. For instance, Genorio *et al.*[16] proposed a method to graft soluble electrochemically active organic materials onto the surface of insoluble substrates (*i.e.* silica and carbon black). Song *et al.*[21] proposed a series of polymer–graphene nanocomposites as ultrafast-charge and discharge cathodes for lithium batteries. The highly dispersed graphene sheets in the nanocomposites enhanced the electrochemical activity of the polymer cathode. However, one drawback of this approach is while it improves the cycling stability, the specific capacity of the electrode materials is reduced due to the increased weight and the volume of the composite. Another effective approach is to minimize the solubility of the materials through polymerization or cyclization. Song and co-workers[12] prepared dianhydrides-based polymers, namely polyimides (PIs), as cathodes by the polymerization of the redox active organic building block (*i.e.* pyromellitic dianhydride (PMDA) and 1,4,5,8-naphthalenetetracarboxylic dianhydride (NTCDA)) and the electrochemically inert linker (*i.e.* *p*-phenylenediamine (*p*PDA) and ethylene diamine (EDA)). The polymer electrodes exhibit a maximum specific capacity of 170–200 mA h g^{-1} at the rate of 1/20C and improved cycling performance compared with the dianhydride precursors. Recently, Chen *et al.*[22] synthesized a molecular triangular prism of (−)-NDI-Δ through cyclization of NTCDA and (*RR*)-*trans*-1,2-cyclohexanediamine (*t*CHDA). Besides its chemical stability,

[a] *SZU-NUS Collaborative Innovation Center for Optoelectronic Science & Technology, Key Laboratory of Optoelectronic Devices and Systems of Ministry of Education and Guangdong Province, College of Optoelectronic Engineering, Shenzhen University, Shenzhen 518060, China. E-mail: chmlohkp@nus.edu.sg, chmsuc@hotmail.com*

[b] *Department of Chemistry, Centre for Advanced 2D Materials (CA2DM) and Graphene Research Centre, National University of Singapore, 3 Science Drive 3, Singapore 117543, Singapore*

† Electronic supplementary information (ESI) available. See DOI: 10.1039/c6mh00072j

‡ These authors contributed equally.

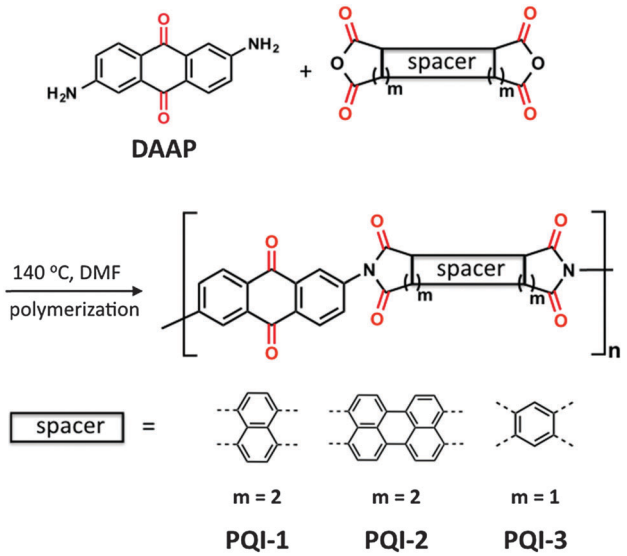

Scheme 1 Synthesis of polyquinoneimines (PQIs) by condensation polymerization.

the rigid naphthalenediimide nanoporous molecular triangle enhanced the electronic properties, leading to an ultrahigh rate capability and good cycling performance. Although these approaches could solve the dissolution problem, the inadvertent introduction of redox inert linkers (*i.e.* *p*PDA, EDA and *t*CHDA) increased the molar mass and reduced the theoretical specific capacity of electrochemically active organic molecules.[12,22–27] In this regard, we propose the usage of a electrochemically active linker to construct the organic electrodes to overcome this trade-off issue between electrolyte stability and preservation of high specific capacity.

In this study, a redox-active organic molecule, 2,6-diaminoanthraquinone (DAAP) was selected as a linker to connect the anhydrides into polyquinoneimines (PQIs) *via* a facile wet-chemistry approach (Scheme 1). As both quinones and anhydrides are electrochemically active, the direct polymerization of these two monomers did not introduce additional inactive monomers, thus minimizing the loss of theoretical specific capacity with respect to the molar mass increase. Furthermore, the increased molar mass effectively suppresses the dissolution of the active materials in the electrolyte. PQIs synthesized using this unique polymerization strategy can realize a high capacity as well as a good cycle stability, which makes PQIs a promising organic positive-electrode material for lithium ion batteries.

Experimental

All the starting materials (DAAP, NTCDA, PTCDA, PMDA) were purchased from Sigma Aldrich. The PQIs were synthesized *via* a DMF solution process at 140 °C under a N_2 atmosphere for 3 or 7 days. The organic positive-electrodes were fabricated using the following procedure. The active material, Super P and the polyvinylidene fluoride (PVDF) binder were mixed in a ratio of 45 : 45 : 10 (45 wt% active material) in *N*-methyl-2-pyrrolidone (NMP) to form a well-dispersed slurry by stirring overnight and then coated onto an aluminum foil substrate. Coatings were dried immediately in a blast oven at 80 °C for about 2 h, followed by activation in a vacuum oven at 80 °C for 24 h to produce membranes that were then cut into circular electrode discs with a diameter of 14 mm. After weighing the electrode discs (active material loading: ~1 mg cm^{-2}), the cells were assembled in a glovebox (VAC) under an Ar atmosphere with H_2O and O_2 contents lower than 1 ppm, using CR2016 coin cell hardware, with lithium foil as the counter electrode and Whatman Glass Microfibre Filter as the separator. The electrolyte contains 1 M lithium bis(trifluoromethanesulfonyl)imide (LiTFSI) in a mixed solvent of 1,3-dioxolane (DOL) and 1,2-dimethoxyethane (DME) (1 : 1 v/v).

Cyclic voltammetry (CV) was performed using an Ivium-n-Stat multi-channel electrochemical analyser. Cyclic voltammograms were recorded over the potential range of 1.5–3.5 V at a scanning rate of 0.1 mV s^{-1}, starting from OCP to the cathodic scan (discharge) direction. Galvanostatic discharge–charge cycling of the batteries was monitored within a voltage window of 1.5–3.5 V using a LAND Battery Tester. All potentials hereafter are given *versus* Li/Li^+. All the electrochemical measurements were performed at room temperature.

For chemical analyses, the PQI electrodes were subjected to different states of galvanostatic discharge–charge. The cells were disassembled and the samples were rinsed with ReagentPlus® 1,3-dioxolane (DOL, 99%, Sigma-Aldrich) and dried under an Ar flow for Fourier transform infrared spectroscopy (FTIR, transmission mode, OPUS/IR PS15 spectrometer, Bruker) analyses. SEM and TEM imaging of PQIs pristine materials were performed using a JEOL JSM-6701F Field-Emission Scanning Electron Microscope (FESEM) and a JEOL JEM-3011 Transmission Electron Microscope (TEM).

Results and discussion

The PQIs were synthesized *via* a facile *N*,*N*-dimethylformamide (DMF, anhydrous) solution-based polycondensation reactions of dianhydrides with DAAP. The polycondensation reactions have been widely used previously.[6,21,25,28] The products were characterized by FTIR spectroscopy (Fig. 1 and Fig. S1, ESI†) and all the characteristic peaks are summarized in Table S2 (ESI†). A new peak at ~1360 cm^{-1} in all the PQIs ascribed to the stretching vibration of the C–N bond appeared, and the characteristic absorbance bands at 3332 and 3423 cm^{-1} assignable to the stretching vibration of $-NH_2$ bonds in DAAP diminished, which indicates that DAAP and dianhydride monomers were linked successfully by polymerization. Furthermore, the characteristic of C═O related bands in the monomer precursors shifted after the polymerization due to the formation of extended π conjugation.[23–27] Typically, the characteristic absorption peaks of the NTCDA (at 1764 and 1728 cm^{-1}) and the DAAP (at 1659 and 1627 cm^{-1}) monomer, corresponding to asymmetric and symmetric stretching vibration of C═O bonds, shifted to 1713 and 1672 cm^{-1} in the PQI-1, respectively. All these pieces of evidence

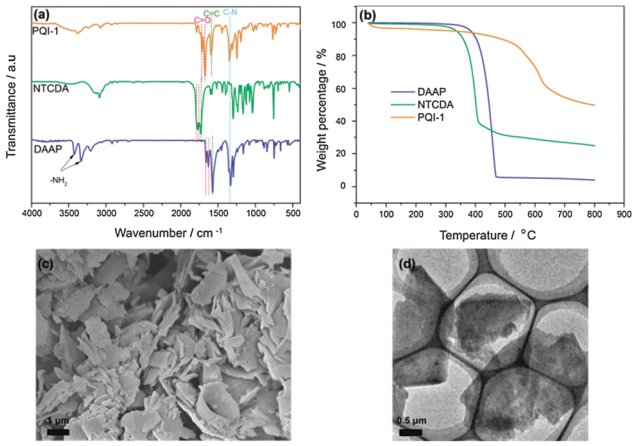

Fig. 1 (a) FTIR curves and (b) TGA of PQI-1 and its precursors (DAAP and NTCDA), (c) SEM and (d) TEM images of PQI-1.

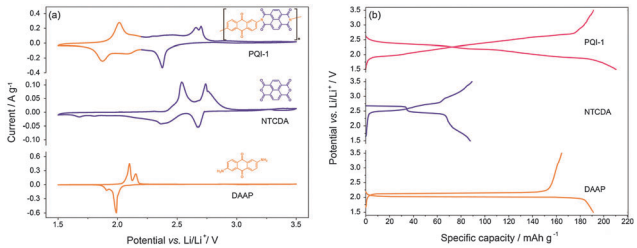

Fig. 2 (a) The first CV curves (scan rate: 0.1 mV s^{-1}) and (b) the first discharge–charge curves of the DAAP, NTCDA and PQI-1 in the 1.5–3.5 V potential range.

suggested the successful synthesis of the target PQIs *via* polymerization. Thermal gravimetric analysis (TGA, Fig. 1b) shows that the decomposition onset of PQI-1 occurs from 500 °C in the N_2 atmosphere, much higher than the decomposition onset of NTCDA and DAAP. This further suggests that PQI-1 has a better thermal stability compared with its precursors, which is beneficial from an operational safety viewpoint. Scanning Electron Microscopic (SEM) and Transmission Electron Microscopic (TEM) images of PQI-1 show that it has a lamellar structure (Fig. 1c and d) after polymerization.

The electrochemical performance of the PQIs is investigated by utilizing the CR2016 coin cell, in which the cathode is prepared by mixing PQIs as active materials (45 wt%) with a conductive additive (Super P, 45 wt%) and the polyvinylidene fluoride binder (PVDF, 10 wt%). In order to exploit the lithium storage properties of PQIs, the PQI-1 together with its precursors (DAAP and NTCDA) are studied thoroughly. The electrochemical properties of PQI-2 and PQI-3 are presented in the ESI.† The cyclic voltammograms (CVs) and the galvanostatic discharge–charge profiles of the PQI-1 electrode and its precursors (DAAP and NTCDA) during their first cycle are shown in Fig. 2. The first CV cycle of DAAP presents two pairs of redox peaks centred at ~2.1 V, corresponding to the two electron reactions of the carbonyl groups in DAAP. The CV curves of NTCDA also present two pairs of peaks, but centred at a higher potential of ~2.6 V. Since two different carbonyl groups are derived from the DAAP and NTCDA moieties, it can be expected that PQI-1 will preserve their respective electrochemical behaviors. Indeed, the CV profiles of PQI-1 show two sets of redox peaks (centred at ~2.0 and ~2.5 V, respectively) attributable to the carbonyl groups from DAAP and NTCDA (Fig. 2a). It is worth mentioning that the redox peak positions of the carbonyl group in NTCDA (2.6 V) is slightly higher than that observed in PQI-1 (2.5 V), indicating the redox potentials of the different carbonyl groups are influenced by the conjugated molecular structure. A slight potential offset between PQIs and their precursors are also observed in the PQI-2 and PQI-3 (Fig. S7, ESI†). The relative intensities of the peaks in the CV curves indicate that PQI-1 exhibits a stronger electrochemical activity compared with NTCDA (0.3 to 0.1 A g^{-1}), but a weaker activity compared to DAAP (0.5 A g^{-1}).

Consistent with the CV results, the charge and discharge behaviors of PQI-1 combine the merits from its respective precursors (DAAP and NTCDA). The initial discharge–charge voltage profiles of PQI-1 and its precursors at a constant current density of 100 mA g^{-1} and in the potential range of 1.5–3.5 V (*vs.* Li/Li^+) are shown in Fig. 2b. The DAAP electrode material exhibits a discharge and charge plateau at *ca.* 2.0 V, giving an initial capacity of 191.3 and 164.4 mA h g^{-1} for discharge and charge processes, respectively. For the NTCDA, two discharge plateaus at about 2.68 and 2.45 V can be observed, which can be attributed to the two-step process of lithiation with an initial capacity of 87.7 and 89.2 mA h g^{-1} for discharge and charge processes, respectively, as demonstrated by CV. With an average potential of ~2.3 V, PQI-1 exhibits discharge and charge capacities up to 210 and 190 mA h g^{-1}, respectively, thus affording higher specific capacities compared with its monomer parts. The sloping profiles of PQI-1 further indicate the reduction of energy barrier between two different carbonyl groups upon polymerization, which is in agreement with the observation of its CV profiles.

The redox mechanism of PQI-1 with lithium is investigated using FTIR spectroscopy during battery lithiation and delithiation (Fig. 3), carried out in a vacuum. The cells were disassembled at the lithiation (discharged to 1.5 V) and delithiation (recharged to 3.5 V) states in a glovebox to prepare the testing pellet. For the pristine electrode materials, the IR absorbance signal at 1593 cm^{-1} can be attributed to the vibration of the C=C bonds in PQI-1. With the sample discharged to 1.5 V, two new absorbance signals at 1514 and 1625 cm^{-1} assigned to vibration of C=C bonds emerged as well as a new peak at 1396 cm^{-1} assigned to vibration of C–O bonds appeared, implying the formation of new C=C bonds and C–O–Li bonds in lithiated PQI-1. After charge back to 3.5 V, the peaks at 1514 and 1625 cm^{-1} disappeared and the spectrum returned to a state similar to that of the pristine sample, suggesting the reversible lithiation/delithiation process. The absorbance signals at 1672 and 1713 cm^{-1} assignable to electrochemically active C=O bonds show intensity variation during discharge and charge processes. The IR signal of carbonyl groups originating from the quinone moieties at 1672 cm^{-1} almost disappeared when discharged to 1.5 V, indicating that these serve as redox-active sites. However, the signal intensity of carbonyl groups on the anhydrides (1713 cm^{-1}) only decreases

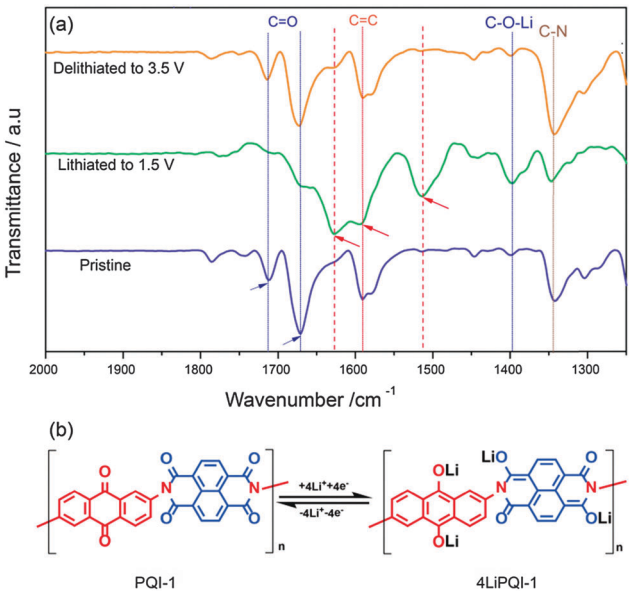

Fig. 3 (a) FTIR spectra of the PQI-1 electrode at different states of lithiation/delithiation (pristine, lithiated to 1.5 V and delithiated to 3.5 V); (b) proposed reversible electrochemical redox mechanism of PQI-1 during the lithiation/delithiation process.

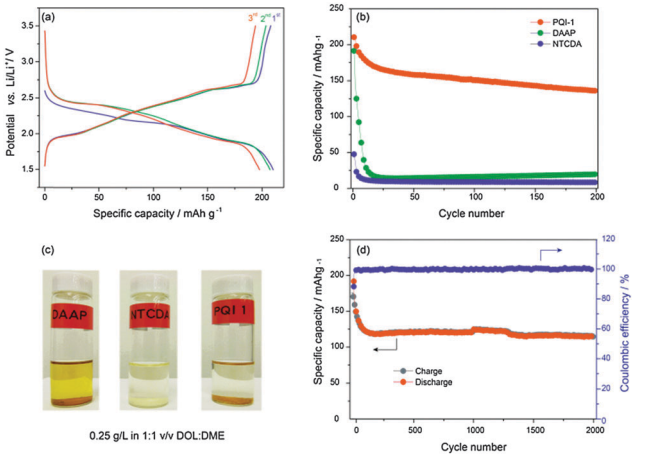

Fig. 4 (a) The discharge–charge curves of PQI-1 and (b) the cycling performance of DAAP, NTCDA and PQI-1 at a current rate of 100 mA g^{-1}; (c) the solubility of DAAP, NTCDA and PQI-1 in a solution (0.25 g L^{-1}) of 1 : 1 v/v DOL:DME; (d) the cycling performance and coulombic efficiency of PQI-1 at a current rate of 1 A g^{-1}.

when discharged, then it increases when recharged, indicating a partial lithiation process of anhydride C═O bonds. The reversible changes of the C═C and C═O bonds vibrational modes in the electrode coincide with the lithiation/delithiation of PQI-1, which evidences the participation of C═O double bonds in the redox reaction. Based on the FTIR studies, the redox mechanism could be deduced, as shown by the chemical equations in Fig. 3b. Two carbonyl groups from quinone moieties participated in the redox reaction of the PQI. However, the conjugated dianhydride unit can only accommodate two electrons during lithiation due to the repulsion between injected negative charges, which is consistent with previous report.[12,15]

As revealed in previous work, the dissolution of organic electrode materials in the electrolytes is one of the main reasons for their poor cycling performance in LIBs.[12,22] For the same reason, the precursors (DAAP and NTCDA) show very poor cycling performance, with their specific capacities decreasing to less than 20 mA h g^{-1} after only a few cycles. However, the PQI-1 electrode presents a high specific capacity of 210.3 mA h g^{-1} in the first discharge process, and retains a capacity of 135.6 mA h g^{-1} even after 200 cycles at a current density of 100 mA g^{-1}, with a capacity retention ratio of 64.5% (Fig. 4b). The solubility of DAAP, NTCDA and PQI-1 in the solution of 1,3-dioxolane (DOL) and 1,2-dimethoxyethane (DME) (1 : 1 v/v), which is used for preparing electrolytes, is shown in Fig. 4c. PQI-1 is only sparingly soluble in the electrolyte solvents compared with the DAAP and NTCDA precursors, which explains the improved cycling performance. Moreover, the conjugated polymer structure of the PQI-1 exhibits a high capacity retention of 67.8% even at a high current density (1 A g^{-1}) after 2000 cycles (Fig. 4d).

The electrochemical behavior of PQI-1 analogues PQI-2 and PQI-3 was also investigated (Fig. S7, ESI†) to obtain further structure–property correlations. From the CV curves of the PQI-2 and PQI-3 (Fig. S7a and b, ESI†), two different redox potentials centered at 2.5 and 2.1 V respectively, are observed due to the different anhydride precursors (PTCDA and PMDA) used in different PQI syntheses. From the discharge–charge curves (Fig. S7c and d, ESI†), the PQI-2 also shows about 0.4 V higher average discharge potential than that of PQI-3. Moreover, the discharge–charge curves show a much larger polarization for PQI-2 (~0.3 V) than that for PQI-3 (~0.1 V) due to the inferior electrochemical activity associated with the larger molecular structure, in agreement with the CV results. Fig. S7e and f (ESI†) show the cycling performances of the PQI-2 and PQI-3. The PTCDA based PQI-2 material presents a capacity increase during the first several cycles, corresponding to an activation process of the polymer.[21,29] After 8 cycles, the PQI-2 electrode presents a stable discharge–charge capacity >100 mA h g^{-1} which is stable up to 200 cycles. However, different from its analogues PQI-1 and PQI-2, the PMDA-based PQI-3 polymer shows a continuous capacity fading in the first twenty cycles (from 136 to 39.8 mA h g^{-1}). Since some side reactions or instabilities may affect the cycling stability,[6,12] the destruction of the conjugate structure of PMDA-based PQI-3 may be responsible for the capacity degradation rather than the dissolution of active materials, in accordance with the previous reports for PMDA and PMDA-based PI.[30–33]

Conclusions

In summary, this work gives important insights into the development of new generation organic cathode materials with high specific capacity and stability through the design and optimization of their molecular structures. The concept of directly polymerizing two electroactive monomers to make a polymer with improved electrolyte stability without sacrificing significant theoretical specific capacity is demonstrated in this work. This simple synthetic strategy should be applicable to a wide class of redox

active monomers which can be polymerized directly, thus opening up an avenue for developing highly stable organic electrode materials for lithium storage.

Acknowledgements

This work was supported by an NRF investigator award: "Graphene Oxide – A new case of catalytic, ionic and molecular sieving materials [R-143-000-610-281]". The authors also acknowledge support from the National Natural Science Foundation of China (Grant No. 21506126 and 51502174), the Science and Technology Planning Project of Guangdong Province (Grant No. 2016B050501005), the Shenzhen Science and Technology Research Foundation (Grant No. JCYJ20150324141711616, JCYJ20150626090504916 and JCYJ20150324141711645) and the China Postdoctoral Science Foundation (2015M572349 and 2015M582401).

Notes and references

1 P. Novák, K. Müller, S. V. Santhanam and O. Hass, *Chem. Rev.*, 1997, **97**, 207.
2 M. Armand and J.-M. Tarascon, *Nature*, 2008, **451**, 652.
3 P. Poizot and F. Dolhem, *Energy Environ. Sci.*, 2011, **4**, 2003.
4 Y. Liang, Z. Tao and J. Chen, *Adv. Energy Mater.*, 2012, **2**, 742.
5 Z. Song and H. Zhou, *Energy Environ. Sci.*, 2013, **6**, 2280.
6 B. Häupler, A. Wild and U. S. Schubert, *Adv. Energy Mater.*, 2015, **5**, 1402034.
7 H. Chen, M. Armand, G. Demailly, F. Dolhem, P. Poizot and J.-M. Tarascon, *ChemSusChem*, 2008, **1**, 348.
8 H. Chen, M. Armand, M. Courty, M. Jiang, C. P. Grey, F. Dolhem, J.-M. Tarascon and P. Poizot, *J. Am. Chem. Soc.*, 2009, **131**, 8984.
9 M. Armand, S. Grugeon, H. Vezin, S. Laruelle, P. Ribière, P. Poizot and J.-M. Tarascon, *Nat. Mater.*, 2009, **8**, 120.
10 Z. Song, H. Zhan and Y. Zhou, *Chem. Commun.*, 2009, 448.
11 W. Walker, S. Grugeon, O. Mentre, S. Laruelle, J.-M. Tarascon and F. Wudl, *J. Am. Chem. Soc.*, 2010, **132**, 6517.
12 Z. Song, H. Zhan and Y. Zhou, *Angew. Chem., Int. Ed.*, 2010, **49**, 8444.
13 X. Han, C. Chang, L. Yuan, T. Sun and J. Sun, *Adv. Mater.*, 2007, **19**, 1616.
14 H. P. Wu, Q. Yang, Q. H. Meng, A. Ahmad, M. Zhang, L. Y. Zhu, Y. G. Liu and Z. X. Wei, *J. Mater. Chem. A*, 2016, **4**, 2115.
15 K. C. Kim, T. Liu, S. W. Lee and S. S. Jang, *J. Am. Chem. Soc.*, 2016, **38**, 2374–2382.
16 B. Genorio, K. Pirnat, R. Cerc-Korosec, R. Dominko and M. Gaberscek, *Angew. Chem., Int. Ed.*, 2010, **49**, 7222.
17 Y.-X. Yu, *J. Mater. Chem. A*, 2014, **2**, 8910.
18 Y.-X. Yu, *ACS Appl. Mater. Interfaces*, 2014, **6**, 16267.
19 F. Xu, S. Jin, H. Zhong, D. Wu, X. Yang, X. Chen, H. Wei, R. Fu and D. Jiang, *Sci. Rep.*, 2015, **5**, 8225.
20 J.-K. Kim, Y. Kim, S. Park, H. Kob and Y. Kim, *Energy Environ. Sci.*, 2016, DOI: 10.1039/c5ee02806j.
21 Z. Song, T. Xu, M. L. Gordin, Y.-B. Jiang, I.-T. Bae, I. Q. Xiao, H. Zhan, J. Liu and D. Wang, *Nano Lett.*, 2012, **12**, 2205.
22 D. Chen, A.-J. Avestro, Z. Chen, J. Sun, S. Wang, M. Xiao, Z. Erno, M. M. Algaradah, M. S. Nassar, K. Amine, Y. Meng and J. F. Stoddart, *Adv. Mater.*, 2015, **27**, 2907.
23 H. Wu, K. Wang, Y. Meng, K. Lua and Z. Wei, *J. Mater. Chem. A*, 2013, **1**, 6366.
24 H. Wang, S. Yuan, D. Ma, X. Huang, F. Meng and X. Zhang, *Adv. Energy Mater.*, 2014, **4**, 1301651.
25 W. Luo, M. Allen, V. Raju and X. Ji, *Adv. Energy Mater.*, 2014, **4**, 1400554.
26 H. Wu, Q. Meng, Q. Yang, M. Zhang, K. Lu and Z. Wei, *Adv. Mater.*, 2015, **27**, 6504.
27 J. Wu, X. Rui, C. Wang, W.-B. Pei, R. Lau, Q. Yan and Q. Zhang, *Adv. Energy Mater.*, 2015, **5**, 1402189.
28 Y. Wu, S. K. Mohan Nalluri, R. M. Young, M. D. Krzyaniak, E. A. Margulies, J. F. Stoddart and M. R. Wasielewski, *Angew. Chem., Int. Ed.*, 2015, **54**, 1.
29 W. Xu, A. Read, P. K. Koech, D. Hu, C. Wang, J. Xiao, A. B. Padmaperuma, G. L. Graff, J. Liu and J.-G. Zhang, *J. Mater. Chem.*, 2012, **22**, 4032.
30 S. Renault, J. Geng, F. Dolhem and P. Poizot, *Chem. Commun.*, 2011, **47**, 2414.
31 S. Renault, V. A. Mihali, K. Edström and D. Brandell, *Electrochem. Commun.*, 2014, **45**, 52.
32 K. Oyaizu, A. Hatemata, W. Choi and H. Nishide, *J. Mater. Chem.*, 2010, **20**, 5404.
33 Y. Meng, H. Wu, Y. Zhang and Z. Wei, *J. Mater. Chem. A*, 2014, **2**, 10842.